Materials Science-Poland, *Vol. 27*, *No. 3*, *2009*

Ambipolar injection into pentacene field effect transistor observed by time-resolved optical second harmonic generation imaging*

T. MANAKA**, M. NAKAO, E. LIM, M. IWAMOTO

Department of Physical Electronics, Graduate School of Science and Engineering,
Tokyo Institute of Technology, 2-12-1 Ookayama, Meguro-ku, Tokyo 152-8552, Japan

Ambipolar carrier injection from gold electrode into pentacene was investigated by time-resolved optical second harmonic generation (TRM-SHG) imaging. Smooth hole injection is verified by rapid decrease of the SHG intensity at the electrode edge, indicating the absence of an injection barrier. In contrast, TRM-SHG results clearly indicated the presence of electron injection from the high-work function metal into the electrode, though after injection electrons were trapped in the channel and could not contribute to the conduction. Transient electric field distribution due to the injected holes and electrons were evaluated based on the SHG intensity distribution.

Key words: *optical second harmonic generation (SHG); organic field effect transistor; carrier injection*

1. Introduction

For organic electronic devices such as organic field effect transistors (OFETs), device operation is ruled by the injection, accumulation and transport processes of a carrier. In this sense, metal–semiconductor contacts play an important role in organic electronic devices, because injected carriers dominate the device operation [1]. For instance, ambipolar behaviour in OFETs was observed upon using appropriate electrode metals: electrons and holes are selectively injected from the electrode with a low and a high work function, respectively [2–4], clearly showing the significance of electrode contact. In contrast, for Si and other inorganic semiconductors, intentional doping precisely determines the type of majority carrier and carrier density in the semiconductors, and thus the injection and transport processes can be fully controlled.

---

*The paper presented at the 11th International Conference on Electrical and Related Properties of Organic Solids (ERPOS-11), July 13–17, 2008, Piechowice, Poland.

**Corresponding author, e-mail: manaka@ome.pe.titech.ac.jp

Owing to the irregularities of the metal–organic interface, the situation becomes more complicated for organic devices, and adequate control of injection and transport processes is not satisfactory at present. It was reported that the preparation process of a metal electrode significantly affects properties of the device [5]. Therefore, an adequate evaluation and control of injection processes is of great importance to improve device performance effectively.

For pentacene FETs, holes inject smoothly from Au electrode because the energy level of the highest occupied molecular orbital (HOMO) in pentacene [6] is close to the work function of Au [7]. On the other hand, since an electron should be injected into the lowest unoccupied molecular orbital (LUMO), the metal with a low work function such as Ca and Mg is suitable for electron injection into pentacene [2]. In this way, use of an appropriate electrode is a general way to realize the ambipolar operation in OFET. Nevertheless, we reported the presence of the electron injection from Au electrode into pentacene FET observed by the electric field induced optical second harmonic generation (EFISHG) [8]. In the present paper, ambipolar carrier behaviour in pentacene FET is reported based on results of time resolved, optical second harmonic generation (TRM-SHG). In our previous paper, TRM-SHG measurement was introduced for visualizing carrier motion in OFETs based on the EFISHG [9]. Since the SHG signal is activated by an electric field applied to organic materials [10, 11], carrier motion can be observed by following the time evolution of the electric field distribution in the devices because charges are the source of a local electric field. One of the important advantages of the TRM-SHG method is the capacity to discriminate the injection and transport processes in devices. By using this technique, injection of an electron from noble metals such as Au into pentacene is revealed, and the motion of both carriers in pentacene FET is visualized with a high spatial resolution lower than 1 μm. Furthermore, we introduce the method of evaluation of transient electric field distribution in OFET by analyzing the TRM-SHG results. Quantitative analysis of the time-dependent electric field distribution would be helpful for subsequent discussion regarding the device operation mechanism.

2. Experimental

The samples used in the experiments were top-contact pentacene FETs. Heavily doped Si wafers covered with a 500 nm thick oxide (SiO_2) layer were used as the base substrate. Before the pentacene deposition, a 100 nm thick poly(methyl methacrylate) layer (PMMA) was spin-coated in order to improve the on-off ratio of the devices. Then, the pentacene layer, approximately 100 nm thick, was deposited on a surface. The process pressure during deposition of pentacene was kept at less than 1×10^{-4} Pa, and the deposition rate was controlled at approximately 3 nm/min. After the deposition of pentacene, top-Au electrodes (source and drain electrodes) 100 nm thick were deposited. The designed channel length (L) and width (W) were 50 μm and 3 mm,

respectively. Pentacene FETs were operated with the application of pulse voltages using a function generator (NF Corp., WF1947) and a high speed bipolar amplifier (NF Corp., HSA4101). All measurements were performed in laboratory ambient atmosphere.

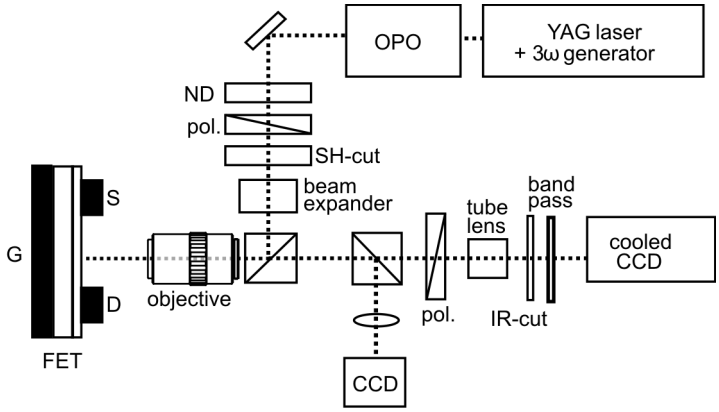

Fig. 1. Optical configuration of the TRM-SHG measurement. Wavelength of the SHG measurement can be changed using OPO, and fundamental light with the wavelength of 1120 nm was chosen in this experiment [12]. The fundamental light is focused on the device using a microscopic objective lens

The light source for the TRM-SHG measurement was an optical parametric oscillator (OPO: Continuum Surelite OPO) pumped by the third-harmonic light of a Q-switched Nd-YAG laser (Continuum:Surelite II-10). An external Q-switch signal from a YAG laser was also supplied from a function generator to synchronize the voltage pulse applied to the OFET with the laser pulse. A timing chart of the voltage pulse applied to the OFET and of the laser pulse is presented in [10]. Fundamental light was focused onto the channel region of OFET with normal incidence using a long working distance objective lens (Mitutoyo: M Plan Apo SL20×, NA = 0.28, W.D. = 30.5 mm). The fundamental light irradiated a large area (spot size was approximately 150 μm) of the channel region for taking SHG image by using a beam expander (Fig. 1). SH light generated from the FET was filtered by a fundamental-cut filter and an interference filter to remove fundamental and other unnecessary light. Finally, SH light generated was detected by a cooled CCD camera (Andor technology: DU420-BV). In this configuration, the polarization direction of the fundamental light was chosen in the direction corresponding to the channel direction (source-drain direction).

3. Results and discussion

3.1. Hole injection

Figure 2 represents the SHG images from an OFET channel captured with various delay times. To take these images, positive pulses were applied to the source elec-

trode. Here, a source electrode is defined as an electrode from which carriers are injected by the applied voltage pulse. As shown, the SHG peak moves rapidly from the source to the drain electrode with an increase of delay time. It should be noted that no SHG signal was observed from the FET without the pentacene layer. Needless to say, such a device does not show any FET characteristics, though the SiO_2 insulator is subjected to an external electric field. Thus the SHG signal from the gate insulator is negligibly small and the SHG signal from the pentacene layer was selectively observed. In our previous paper, it was shown that migration of the peak position of the SHG intensity follows a novel, diffusion-like behaviour; namely, the square of the peak position of $\bar{x}$ is proportional to time t [13]. As just described, the time-resolved measurement successfully demonstrated the emission band movement of the SHG.

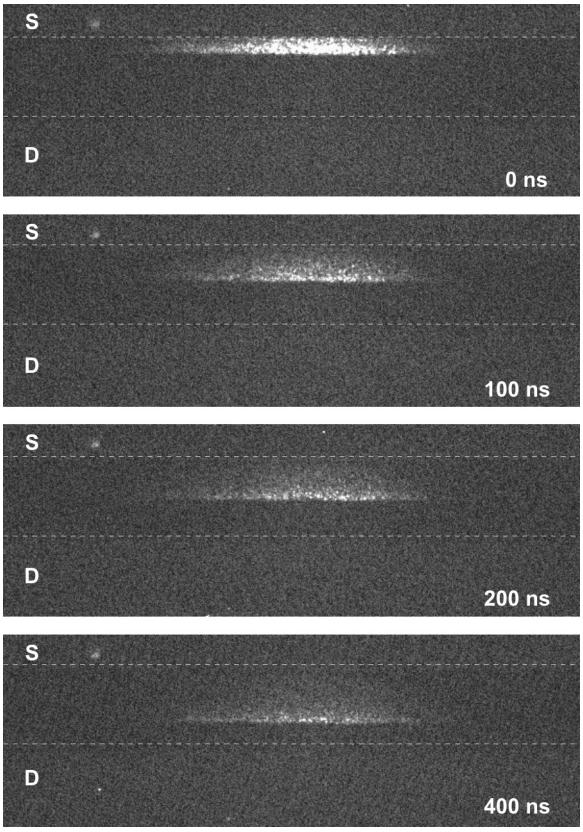

Fig. 2. SHG images from OFET channel with various delay times under the application of positive pulse to the source electrode. These images are top-view of pentacene OFET, the region between two dashed lines corresponds to the channel of the FET. Actual channel length was 45 μm. S and D represent the source and drain electrode, respectively

For hole injection, the injected holes from the source electrode spread immediately over the FET channel. It should be noted that SH intensity immediately disappears

(actually it takes less than 100 ns) at the electrode edge: this indicates a low injection barrier for holes between the Au and the pentacene. After carrier injection, carriers adequately accumulate in the channel. Sufficiently accumulated charges in the channel form the space charge field that cancels out the source field, so that no SHG signal is generated from the edge of the source electrode. Disappearance of the SHG signal around the electrode clearly supports this assertion, that is, no electric field is concentrated at the edge of the electrode. Under our experimental condition, vacuum evaporated pentacene film is composed of a number of small-size domains (domain size was less than 1 μm), and the *a*- and *b*-axis of pentacene crystals align parallel to the substrate surface [14], that is the *c*-axis almost aligns normally to the surface. In that case, electronic conduction is dominated along in-plane direction [15], reflecting strong intermolecular interaction along the *ab* direction. Therefore, it is reasonable to consider that $\chi^{(3)}$ components of pentacene film along the *c*-axis are small compared with that along the in-plane direction. Consequently, the SHG signal is sensitive to the in-plane components of the electric field in pentacene film under the normal incidence condition.

3.2. Electron injection

Figure 3 shows the SHG images from an OFET channel with various delay times associated with an applied negative pulse. To capture these images, negative pulses were applied to the source electrode. It was found that the emission band of the SHG slightly moved away from the source electrode, as shown in the figure. This result indicates that electron injection from the Au electrode to pentacene film was actually possible. Since the energy difference between the LUMO of pentacene the and Fermi level of Au is approximately 2.0 eV [6], electron injection is quite difficult and it is reasonable to consider that electron injection from Au into pentacene is not possible. Metal deposition onto the pentacene layer leads to the penetration of metal atoms into the pentacene layer [5]. Such penetration of metal results in appearance of the interfacial states near the pentacene–Au interface. For hole injection with negligible injection barrier, such interfacial states must prevent the injection, and lead to the degradation of device parameters, such as field effect mobility. However, these interfacial states presumably accept electrons via a tunnelling process from the Au surface. Electron injection, which is strongly inhibited by the energy difference between the LUMO of pentacene and the Fermi level of Au, is presumably promoted under the presence of such states.

Another possible mechanism for the electron injection is the interface dipole layer at the pentacene–Au interface. Formation of the interface dipole layer at the pentacene –Au interface was revealed using UPS measurement in [16], and such an interface dipole supposedly promotes electron injection. As well as at the pentacene–Au interface, UPS measurement also confirmed the presence of the interface dipole at the pentacene–Ag interface. For the Ag electrode, the work function of an Ag surface is lower than that of a Au surface, leading to a more efficient injection of electrons from the Ag

electrode. It should be noted that such electron injection was not observed in the devices using an Ag electrode by the TRM-SHG measurement obtained within the constraints of our experiments. In this sense, penetration of metal atoms into the pentacene layer is more possible for the electron injection. However, at the present stage, the true mechanism of electron injection is not clear. To reveal the details of electron injection such as the mechanisms is our future task.

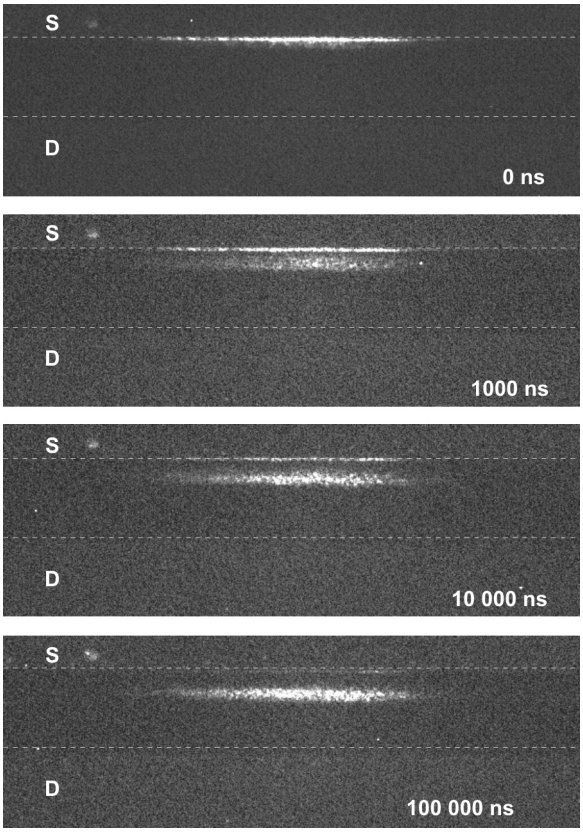

Fig. 3. SHG images from OFET channel with different delay times under the application of a negative pulse to the source electrode. At the edge of source electrode, SH signal still remains at a delay time of 10 μs, though it disappears at the delay time of 100 μs

Interestingly, after the electron injection, motion of the emission band of the SHG stopped immediately near the source electrode (see Fig. 3). Needless to say, it moved smoothly and continuously along the channel for hole injection as a positive pulse was applied (see Fig. 2). These results imply that injected electrons were trapped near the electrode in the FET channel. Benzocyclobutene (BCB) and PMMA layer inserted between organic semiconductor and insulator is frequently used to prevent the electron entrapment [3]. In the present study, PMMA was coated on the SiO_2 surface but the trapping of electrons is actually observed, presumably owing to the presence of oxy-

gen [17, 18] and moisture. Although the electron trapping at the organic semiconductor/insulator interface has been commonly discussed, there is as yet no detailed understanding of such traps. This is the first time to directly observe the interruption of the electron transport. Such observation certainly might help with solving the problem of carrier transport inhibition.

3.3. Electric field distribution

Quantitative evaluation of the transient electric field distribution is introduced, based on the analysis of the SH intensity distribution. For the discussion of the device mechanisms of OFET with the TRM-SHG measurement, some of the most important information which can be extracted from the TRM-SHG results is the time evolution of the electric field and the carrier distribution along the FET channel.

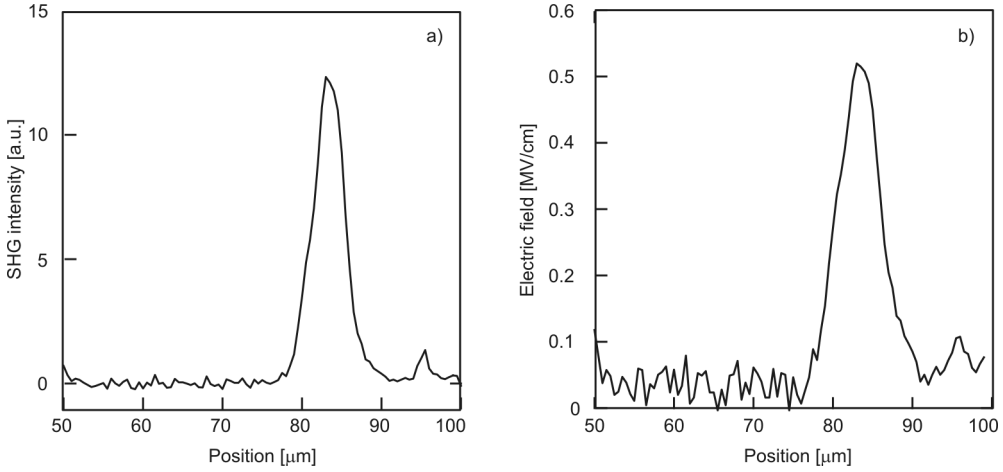

Fig. 4. Typical example of the SH intensity distribution along the FET channel (a) obtained by taking a cross section of an SH image shown in Fig. 3. SH intensity distribution under the electron injection at the delay time of 100 μs is indicated, and electric field distribution along the FET channel (b) evaluated from an SH intensity distribution

In Figure 4, an exemplary SH intensity distribution along the FET channel obtained by taking a cross section of an SH image shown in Fig. 3 (for electron injection, at the delay time of 100 μs), and the distribution of the lateral component of the electric field in the FET channel, respectively. Since SHG intensity is proportional to the square of the local electric field for the EFISHG process, electric field distribution can be obtained with a high spatial resolution by only taking the square root of the SHG distribution. Note that the absolute value of the electric field strength cannot be obtained directly from the SHG intensity. Nevertheless, we can evaluate the electric field strength by comparing it with the result of a reference measurement. Without carrier injection, a Laplace electric field is formed in the devices under the voltage applied to

the electrode. In that case, electric field distribution can be calculated based on the classical electromagnetic theory, taking into account the device geometry [19]. Thus, comparing the theoretical electric field strength with the SHG intensity, the electric field distribution in the devices can be experimentally evaluated.

In a Laplace electric field, the electric field is concentrated between source and gate electrodes, and, accordingly, the peak position of the electric field is located at the edge of the source electrode. In contrast, the peak position of the electric field moves away from the source electrode and is located between the source and drain electrodes after electron injection (see Fig. 4b). This fact clearly indicates that the electric field, after electron injection, is dominated by the space charge field due to the injected electrons. The TRM-SHG measurement can evaluate the transient electric field in devices at high spatial (approximately 1 μm) and temporal (10 ns) resolutions.

4. Conclusion

Ambipolar carrier injection from gold electrode into pentacene was investigated by time-resolved, optical second harmonic generation (TRM-SHG) imaging. Although electron injection from Au into pentacene is quite difficult, because the energy difference between the LUMO of pentacene and the Fermi level of Au is approximately 2.0 eV, TRM-SHG results clearly indicated the electron injection from high-work function metal into pentacene. For this electron injection, motion of the emission band of the SHG stopped in the channel, indicating that the injected electrons were trapped in the OFET channel. A transient electric field, due to injected electrons, was evaluated based on the SHG intensity distribution.

Acknowledgement

This work is supported by the New Energy and Industrial Technology Development Organization (NEDO). Support by the Grants-in-Aid for Scientific Research (Grants Nos.18686029 and 15206032) is also gratefully acknowledged.

References

[1] OGAWA S., KIMURA Y., ISHII H., NIWANO M., Jpn. J. Appl. Phys., 42 (2003), L1275.
[2] YASUDA T., GOTO T., FUJITA K., TSUTSUI T., Appl. Phys. Lett., 85 (2004), 2098.
[3] CHUA L.L., ZAUMSEIL J., CHANG J.F., OU E. C.W., HO P.K.H., SIRRINGHAUS H., FRIEND R.H., Nature, 434 (2005), 194.
[4] ZAUMSEIL J., FRIEND R.H., SIRRINGHAUS H., Nat. Mater., 5 (2006), 69.
[5] CHO J.H., KIM D.H., JANG Y., LEE W. H., IHM K., HAN J.-H., CHUNG S., Appl. Phys. Lett., 89 (2006), 132101.
[6] KARL N., [In:] *Organic Electronic Materials*, R. Farchioni, G. Grosso (Eds.), Springer, Berlin, 2001, p. 231.
[7] MICHAELSON H.B., J. Appl. Phys., 48 (1977), 4729.
[8] LIM E., MANAKA T., IWAMOTO M., J. Appl. Phys., 101 (2007), 024515.

[9] MANAKA T., LIM E., TAMURA R., IWAMOTO M., Nat. Photonics, 1 (2007), 581.
[10] MANAKA T., LIM E., TAMURA R., YAMADA D., IWAMOTO M., Appl. Phys. Lett., 89 (2006), 072113.
[11] MANAKA T., NAKAO M., YAMADA D., LIM E., IWAMOTO M., Opt. Express, 15 (2007), 15964.
[12] MANAKA T., SUZUE Y., IWAMOTO M., Jpn. J. Appl. Phys., 44 (2005), 2818.
[13] MANAKA T., LIU F., MARTIN W., IWAMOTO M., Phys. Rev. B, 78 (2008), 121302(R).
[14] MINAKATA T., IMAI H., OZAKI M., SACO K., J. Appl. Phys., 72 (1992), 5220.
[15] CHENG Y.C., SILBEY R.J., Da SILVA FILHO D.A., CALBERT J.P., CORNIL J., BREDAS J.L., J. Chem. Phys., 118 (2003), 3764.
[16] WATKINS N.J., YAN L., GAO Y., Appl. Phys. Lett., 80 (2002), 4384.
[17] HADDON R.C., PEREL A.S., MORRIS R.C., PALSTRA T.T.M., HEBARD A.F., FLEMING R.M., Appl. Phys. Lett., 67 (1995), 121.
[18] LAQUINDANUM J.G., KATZ H.E., DODABALAPUR A., LOVINGER A.J., J. Am. Chem. Soc., 118 (1996), 11331.
[19] YAMADA D., MANAKA T., LIM E., TAMURA R., IWAMOTO M., J. Appl. Phys., 103 (2008), 084118.

Received 28 August 2008
Revised 7 February 2009